DOI 10.5012/bkcs.2011.32.8.2599

Energy Transfer from Ethidium to Cationic Porphyrins Mediated by DNA and Synthetic Polynucleotides at Low Binding Densities

Jin-A Jung, Sun Hee Jeon, Sung Wook Han,‡ Gil Jun Lee,‡ In-Ho Bae,† and Seog K. Kim*

Department of Chemistry and †Department of Physics, Yeungnam University, Gyeong-buk 712-749, Korea
**E-mail: seogkim@yu.ac.kr*
‡School of Herb Medicine Resource, Kyungwoon University, Kumi, Gyeong-buk 730-852, Korea
Received May 11, 2011, Accepted June 21, 2011

The fluorescence of ethidium bound to DNA, poly[d(A-T)$_2$], and poly[d(G-C)$_2$] at a [ethidium]/[DNA] ratio of 0.005 was quenched by porphyrins when both ethidium and the porphyrins simultaneously bound to the same polynucleotide. The quenching was tested using the "inner sphere" and the "Förster resonance energy transfer" (FRET) models, with the latter found to contribute, at least in part, to the quenching. *Meso*-tetrakis(*N*-methylpyridinium-4-yl)porphyrin (TMPyP) exhibited a higher quenching and FRET efficiency than *cis*-*bis*(*N*-methylpyridinium-4-yl)porphyrin (BMPyP) for all of the tested DNA and polynucleotides, demonstrating that energy transfer efficiency is affected by the number of positive charges of porphyrins.

Key Words : Energy transfer, Porphyrin, Ethidium, DNA, Polynucleotide, Fluorescence

Introduction

Stacked π-orbitals of DNA base pairs form a good medium of electron transfer,[1] and electron transfer through DNA has been intensively studied for potential applications in biotechnology and nanotechnology.[2-6] The biological importance of understanding charge transport through DNA has been highlighted by the discovery of distance oxidative damage to DNA in cell nuclei.[7,8] In regards to nanotechnology, various nanometer-sized self-assembling molecular wires have been designed using the charge transport in a DNA stem.[9-12] DNA mediated hole transfer has also been studied, because these holes may cause oxidative DNA damage *in vivo*, leading to mutations. Holes generated by one-electron oxidation of DNA can migrate a distance of over 200 Å through the DNA by hopping between the guanine bases.[13-19] Molecular wire, superexchange and hopping models are three mechanisms of DNA-mediated electron/hole transport.[5]

The excited energy of DNA-bound donors can also transfer to acceptors.[20-29] In general, the emission energy level of the donor molecule coincides with the absorption energy level of the acceptor in the DNA mediated excited energy transfer. Therefore, its mechanism is believed to be mainly a Förster type resonance energy transfer.[20-29] The excited energy of 4',6-diamidino-2-phenylindole (DAPI) has been reported to be transferred to DNA intercalating [Ru(1,10-phenanthroline)$_2$dypyrido[3,2-*a*:2',3'-*c*]phenazine]$^{2+}$ at high binding densities.[24-27] DAPI is known to bind at the minor groove of DNA,[30-32] while the latter molecule intercalates from the major groove, as the DAPI saturates the minor groove. Thus, energy transfer eventually occurs across the DNA stem. The efficiency of the energy transfer from DAPI is far higher than predicted by the "sphere of action model" when *meso*-tetrakis(*N*-methylpyridinium-4-yl)porphyrin (hereafter referred to as TMPyP, Figure 1) is used as an acceptor.[28,29] However, fluorescence quenching with *cis*-bis(*N*-methylpyridinium-4-yl)porphyrin (hereafter referred BMPyP, Figure 1), which stacks along DNA and poly[d(A-T)$_2$],[33,34] is less efficient than with TMPyP. For both TMPyP and BMPyP, the concentration of DAPI was high enough to saturate the minor groove of the DNA.

This work reports energy transfers from ethidium to TMPyP and BMPyP mediated by various native and syn-

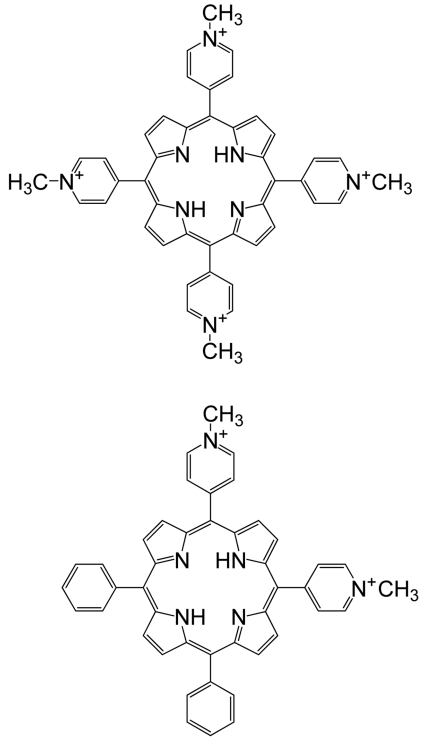

Figure 1. Molecular structures of cationic TMPyP (upper) and BMPyP (lower).

thetic DNAs, namely calf thymus DNA (referred to as DNA), poly[d(G-G)$_2$] and poly[d(A-T)$_2$] at very low binding ratios. Ethidium bromide, which intercalated between the GC and AT base pairs, was used as the energy donor. The acceptor TMPyP intercalated between the base pairs of DNA and poly[d(G-C)$_2$], but it bound across the minor groove of poly[d(A-T)$_2$] at the concentrations adopted this work.[35-37] BMPyP has been previously reported as stacking along the DNA and poly[d(A-T)$_2$], and binding to the outside of poly[d(G-C)$_2$].[33,34] The highest concentration of porphyrins adopted in this work is 2.5 μM, which allows to investigate the energy transfer in DNA and various synthetic polynucelotides at low [drug]/[DNA] ratios.

Experimental

Materials. DNA and synthetic polynucleotides were purchased from Worthington (Lakewood, NJ) and Sigma-Aldrich (Yongin, Korea), respectively. The DNA was dissolved in 5 mM cacodylate buffer containing 100 mM NaCl and 1mM EDTA at pH 7.0 with exhaustive shaking at 4 °C. The mixture was then dialyzed several times against a 5 mM cacodylate buffer at 4 °C. The latter buffer was used throughout this work. Poly[d(G-C)$_2$] and poly[d(A-T)$_2$] were dissolved in 5 mM cacodylate buffer and used without further purification. TMPyP and BMPyP were purchased from Frontier Scientific (Logan, UT) and used without any further purification. The polynucleotide and porphyrins concentrations were spectrophotometrically determined using their extinction coefficients: A_{258nm} = 6700 $cm^{-1}M^{-1}$, A_{257nm} = 8400 $cm^{-1}M^{-1}$, A_{262nm} = 6600 $cm^{-1}M^{-1}$, A_{421nm} = 245000 $cm^{-1}M^{-1}$, and A_{420nm} = 140000 $cm^{-1}M^{-1}$ for DNA, poly[d(G-C)$_2$], poly[d(A-T)$_2$], TMPyP and BMPyP, respectively. The porphyrins were always added last, immediately before measurement, as the mixing order potentially affects the porphyrins' binding mode.[38]

Measurements. Absorption spectra were recorded using a Cary 100 spectrophotometer (Varian, Palo Alto, CA). Circular dichroism (CD) spectra were obtained using either a Jasco J-715 or a J-810 spectropolarimeter (Tokyo, Japan). Both TMPyP and BMPyP are achiral molecules and hence do not produce CD spectra. However, TMPyP induces a clear CD spectrum in the Soret band when it is bound to DNA. This occurs through an interaction between the electric transition moment of the porphyrin and the chirally arranged electric transition moment of the DNA bases. Such induced CD spectra can identify the binding modes of TMPyP to DNA. Fluorescence spectra were recorded using a Jasco FP-777 fluorometer. The fluorescence emission spectra of ethidium in the presence and absence of TMPyP or BMPyP were recorded with an excitation of 527 nm, the maximum excitation for DNA- and polynucleotide-bound ethidium. Excitation and emission wavelengths of 527 nm and 592 nm, respectively, were used in the fluorescence quenching experiment. Fluorescence decay times were measured using an IBH 5000U Fluorescence Life Time System. An LED producing excitation radiation of 493 nm with a full width at half maximum of *ca*. 1.3 ns, was used to excite the DNA-bound ethidium.

The fluorescence quenching of DNA and polynucleotides bound ethidium with TMPyP or BMPyP were analyzed through Stern-Volmer plots.[39]

$$\frac{F_0}{F} = 1 + K_{SV}[Q] \quad (1)$$

In this equation, F_0 and F denote the fluorescence intensities of the fluorophore, DNA-bound ethidium, in the absence and presence of quenchers, respectively. [Q] is the concentration of quencher, TMPyP or BMPyP. The quenching constant, K_{SV}, represents the equilibrium constant for the formation of the nonfluorescent fluorophore-quencher complex in the static quenching process. In the dynamic-collision quenching mechanism, the quenching constant is related to the frequency of collisions and the lifetimes of the excited state of the fluorophore. Upward bending curves in the Stern-Volmer plot are often observed, which may be interpreted in terms of the sphere of action model.

$$\frac{F_0}{F} = (1 + K_D[Q])\exp([Q]VN/1000) \quad (2)$$

Where, K_D is the dynamic quenching constant, and V and N denote the volume of the sphere and Avogadro's number, respectively. The sphere's radius usually coincides with the sum of the molecular radii of the fluorophore and the quencher, the probability of quenching is unity.

When the emission energy level of a fluorophore is superimposed with the absorption energy level of an acceptor, the excited energy of the donor can be directly transferred to the acceptor, known as "Förster type resonance energy transfer (FRET)". The rate of FRET (k_T) from the donor to the acceptor is given by the following equation.[22,23,39]

$$k_T = \frac{1}{\tau_0}\left(\frac{R_0}{r}\right)^6 \quad (3)$$

Where τ_0 denotes the fluorescence decay time of the donor in the absence of the acceptor, and r is the distance between them. The Förster distance at which FRET is 50% efficient, R_0, is related to the spectral overlap between the emission spectrum of the donor and the absorption spectrum of the acceptor ($J(\lambda)$), the relative orientation between the transition dipoles of the donor and the acceptor (κ), the quantum yield of the donor molecule in the absence of the acceptor (Q_D), and the refractive index of the medium (n).

$$R_0 = (J(\lambda)\kappa^2 Q_D n^{-4})^{1/6} \times 8.79 \times 10^{-25} \text{ in cm} \quad (4)$$

where $J(\lambda) = \int_0^\infty F_D(\lambda)\varepsilon_A(\lambda)\lambda^4 d\lambda$

In this equation, $F_D(\lambda)$ is the normalized fluorescence intensity of the donor, and $\varepsilon_A(\lambda)$ denotes the molar extinction coefficient of the acceptor. The energy transfer efficiency, E, is related to the distance through Equation (5), which typically is presented with respect to the measurable quantities F and F_0.

$$E = \frac{R_0^6}{R_0^6 + r^6} = 1 - \frac{F}{F_0} \quad (5)$$

In this work, both the Stern-Volmer and FRET approaches were applied to describe the measured quenching properties of DNA-bound ethidium with TMPyP and BMPyP.

Results

Absorption and CD Spectra of TMPyP and BMPyP Bound to Polynucleotides in the Presence and Absence of Ethidium. Figures 2(a) and (b) show the absorption and CD spectra of TMPyP bound to DNA, poly[d(A-T)$_2$] and poly[d(G-C)$_2$] in the presence and absence of ethidium. The concentrations of nucleobase and TMPyP were 100 μM and 2.5 μM, respectively. The presence of 0.5 μM of ethidium did not alter the spectral properties of the TMPyP-DNA and -polynucleotide complexes, indicating that ethidium and TMPyP bound independently of each other without interfere. The spectra recorded for 0.5, 1.0, 1.5 and 2.0 μM TMPyP were similar when normalized with respect to concentration and hence are not shown. The binding of TMPyP to DNA and poly[d(G-C)$_2$] produce a strong red shift and

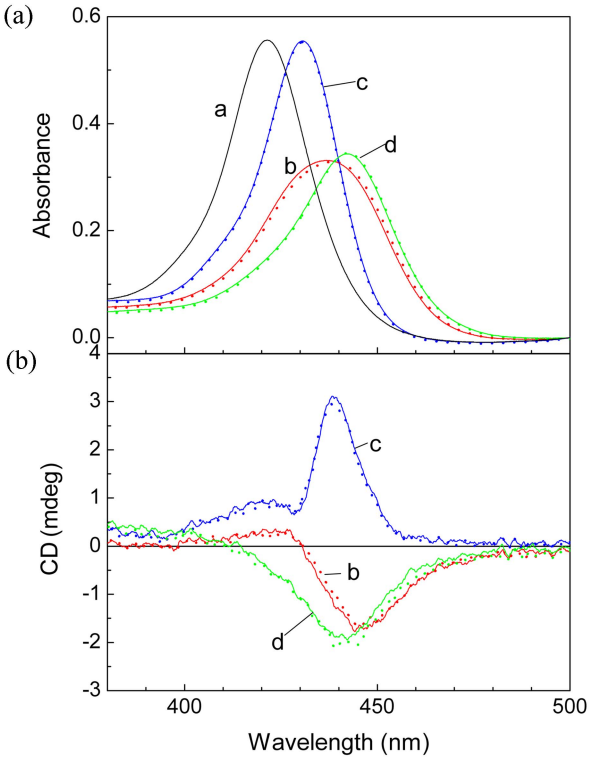

Figure 2. Absorption (panel a) and CD spectra (panel b) of TMPyP bound to DNA (labeled b), poly[d(G-C)$_2$] (labeled c) and poly[d(A-T)$_2$] (labeled d) in the presence and absence of ethidium. The curve a represents the absorption spectrum of TMPyP in the absence of DNA or polynucleotide. The concentrations of TMPyP and DNA were 2.5 μM and 100 μM, respectively. The spectra obtained from [porphyrin] = 0.5, 1.0. 1.5 and 2.0 μM were identical to that at 2.5 μM when the concentration was normalized. The presence of 0.5 μM ethidium did not affect the spectra of DNA-bound TMPyP (dotted curves).

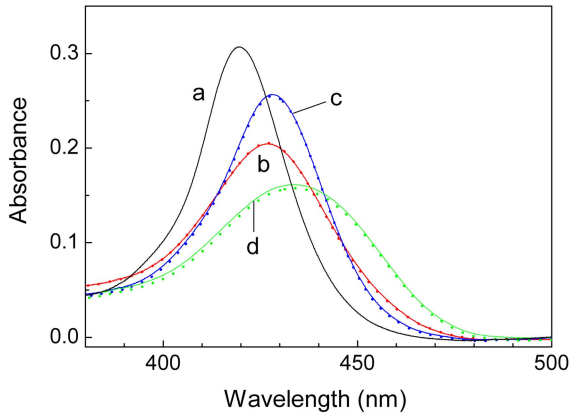

Figure 3. Absorption spectra of BMPyP bound to DNA, poly[d(G-C)$_2$] and poly[d(A-T)$_2$] in the presence and absence of ethidium. The concentrations and curve assignments are as per Figure 2.

hyperchromism in the porphyrin's Soret region. A large negative band in the CD spectra was apparent in the same region. A positive contribution at *ca*. 430 nm also occurred for DNA. Unlike the DNA and poly[d(G-C)$_2$] complexes, the TMPyP-poly[d(A-T)$_2$] complex exhibited vary small hyperchromism and red shift in the absorption spectrum compared with polynucleotide-free TMPyP. The positive CD spectrum in the Soret band suggested that TMPyP mainly bound at the minor groove, probably across the groove.[33-37]

Figure 3 shows absorption spectra of BMPyP bound to DNA, poly[d(G-C)$_2$] and poly[d(A-T)$_2$] in the absence and presence of ethidium. Binding of BMPyP to poly[d(G-C)$_2$] caused the largest hyperchromism: 48.5%, with a 14 nm red shift compared with an absence of DNA. The hyperchromism and red shifts were 16.9% and 8 nm, and 33.2% and 7 nm for poly[d(A-T)$_2$] and DNA, respectively, in accordance with reported values.[33,34] The CD spectrum at these low BMPyP concentrations was extremely weak, as previously reported,[34] and therefore not shown. Polarized spectroscopic study suggested that BMPyP stacked along the stem of the DNA and poly[d(A-T)$_2$] and bound to the outside of poly[d(G-C)$_2$] in a monomeric manner.[34] The presence of ethidium did not alter the spectral properties of BMPyP bound to any of the polynucleotides, similar to TMPyP, suggesting that the simultaneous binding of BMPyP and ethidium to DNA and the synthetic polynucleotides did not affect their binding modes.

The absorption spectra of ethidium in its complexes with DNA and polynucleotides were not altered by the presence of porphyrins (data not shown): the shapes the ethidium's spectra were unaltered when the DNA-porphyrin or polynucleotide-porphyrins absorption was subtracted from the ethidium-DNA (polynucleotide)-DAPI complex. It is also note worthy that the absorption and CD spectrum of porphyrins bound to DNA or polynucleotide were unaffected by the mixing ratio, [porphyrin]/[DNA] when normalized to porphyrin's concentration, suggesting that all porphyrins in the system were bound to DNA or polynucleotide, and that the binding modes were identical at the ratios studied in this work.

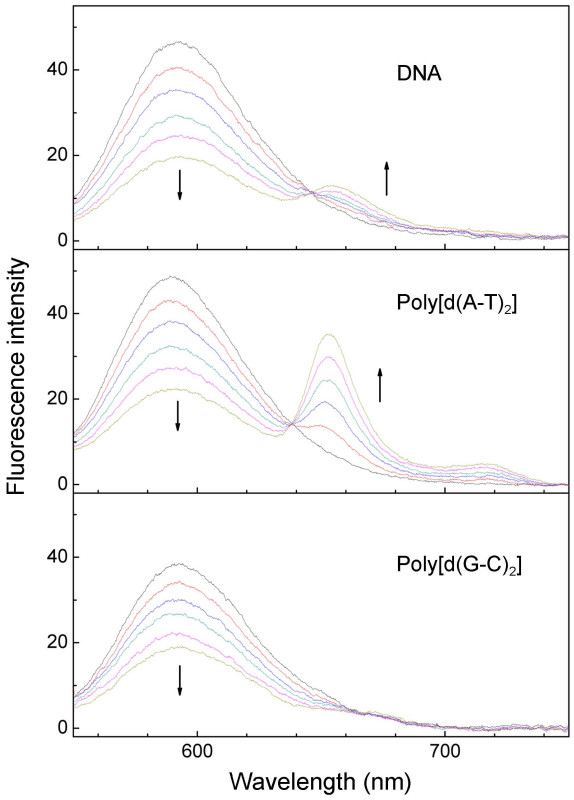

Figure 4. Fluorescence emission spectra of ethidium bound to DNA (panel a), poly[d(A-T)$_2$] (panel b) and poly[d(G-C)$_2$] (panel c) in the presence of 0.0, 0.5, 1.0, 1.5, 2.0, and 2.5 μM TMPyP. The increasing ceoncentration is in the direction of arrows. [DNA] = 100 μM, [ethidium] = 0.5 μM. The emission spectra were recorded at an excitation of 527 nm. Slit widths were 5 nm for both excitation and emission.

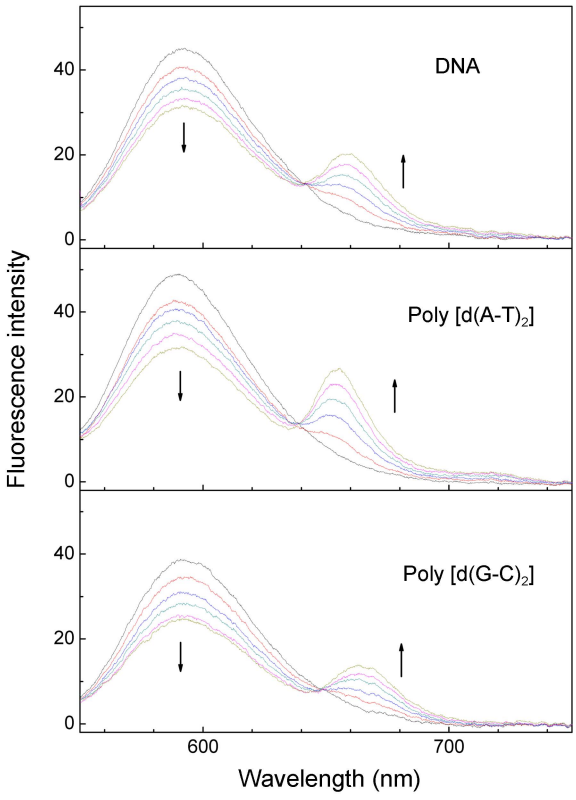

Figure 5. Fluorescence emission spectra of ethidium bound to DNA (panel a), poly[d(A-T)$_2$] (panel b) and poly[d(G-C)$_2$] (panel c) in the presence of BMPyP. The concentrations and conditions are identical to Figure 4.

Quenching of Ethidium Fluorescence by Porphyrins. The effects of increasing concentrations of TMPyP and BMPyP on the fluorescence emission spectra of DNA- and polynucleotide-bound ethidium are shown in Figures 4 and 5. As the concentration of TMPyP or BMPyP increased, the fluorescence intensities of ethidium decreased, but spectra maintained their shapes with maxima at 592 nm. The decrease in fluorescence intensity with increasing TMPyP concentration was accompanied by an increase in the fluorescence intensity at 653 nm for the ethidium-poly[d(A-T)$_2$] complex even though the polynucleotide-ethidium-TMPyP complex was excited in the DNA-bound ethidium excitation region (527 nm). In contrast, a similar increase was not observed with the poly[d(G-C)$_2$] complex. The intensity increase of the emission intensity at 653 nm was very small for the DNA. A similar decrease in fluorescence intensity was found for BMPyP near 592 nm, the emission maximum of polynucleotide-bound ethidium. However, the appearance of emission in the porphyrin emission region contrasted with the TMPyP case. A clear increase in emission intensity with respect to increasing BMPyP concentration was observed for all three polynucleotides. This increase was greatest with poly[d(A-T)$_2$] (Figure 5). In the absence of polynucleotides, ethidium and porphyrin fluorescences were not altered (data not shown), indicating that the changes of ethidium's fluorescence were thoroughly mediated by DNA and the polynucleotides.

Figure 6(a) shows Stern-Volmer plots of the quenching of DNA- and polynucleotides-bound ethidium's fluorescence by TMPyP. The apparent upward bending curves suggest the applicability of the "inner sphere model" (equation (2)). The dynamic quenching constant, K_D, is equivalent to $k_q\tau$, where k_q is the rate of collision between fluorophore and quencher, and τ is the fluorescence decay time of the fluorophore in the presence of the quencher. Sample fluorescence decay times for ethidium bound to DNA are shown in Figure 7. The fluorescence decay profiles of DNA-bound ethidium ([DNA] = 100 μM and [ethidium] = 0.5 μM) were compared in the presence and absence of 2.5 μM TMPyP, with TMPyP clearly affecting the decay profile. The calculated decay time was 22.4 ns without TMPyP; and, 2.17 ns and 19.1 ns with respective amplitudes, a_1 and a_2, of 0.105 and 0.895 with TMPyP. These became 1.92 ns (a_1 = 0.038) and 21.5 ns (a_2 = 0.962) in the presence of 1.0 μM TMPyP. The short decay times observed in the presence of TMPyP reflect either DNA-bound TMPyP or shortened decay time of ethidium by interaction with TMPyP.

The average decay times determined by $(a_1\tau_1^2+a_2\tau_2^2)/(a_1\tau_1+a_2\tau_2)$ were 21.5 ns, 20.7 ns and 18.9 ns in the presence of 0.5 μM, 1.5 μM and 2.5 μM TMPyP, respectively, indicating that the dynamic portion of Equation (2)

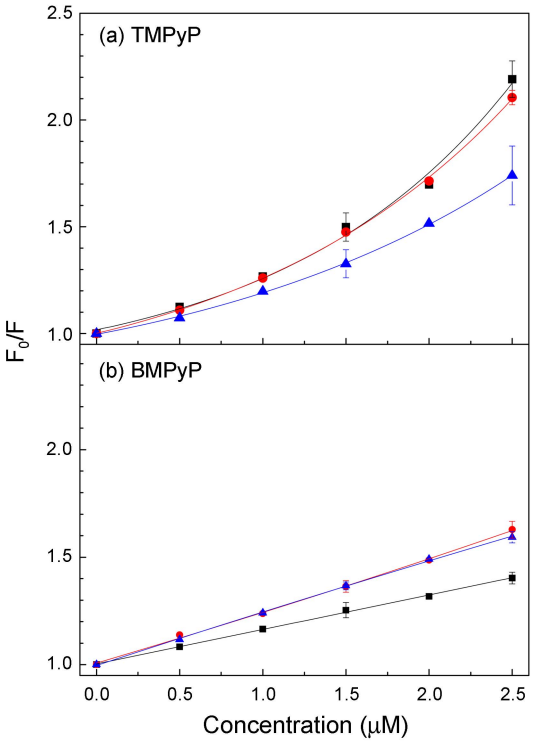

Figure 6. Quenching of the fluorescence intensity of ethidium bound to DNA (squares), poly[d(G-C)$_2$] (triangles), and poly[d(A-T)$_2$] (circles) by TMPyP and BMPyP. The excitation and emission wavelengths were 527 nm and 592 nm, respectively. The slit widths were 5 nm for both excitation and the emission. [DNA] = 100 μM and [ethidium] = 0.5 μM. The error bars indicate the standard deviation from seven measurements.

was negligible. Thus, the Stern-Volmer plot (Figure 6(a)) could be reduced to a simple exponential term.

$$\frac{F_0}{F} = \exp([Q]VN/1000) \quad (6)$$

The best fitting curve using this equation is also shown in the Figure 6(a). Similarly, the decay time of ethidium-poly[d(A-T)$_2$] was 23.8 ns, becoming 1.72 ns (a_1 = 0.036) and 23.8 ns (a_2 = 0.964) in the presence of 1.0 μM TMPyP. For poly[d(G-C)$_2$], the fluorescence decay time was 21.5 ns, becoming 0.47 ns (a_1 = 0.098) and 21.5 ns (a_2 = 0.902) in the presence 1.0 μM TMPyP. The radii of the inner spheres were calculated for ethidium and TMPyP, where quenching efficiency was unity. The radii were similar for DNA and poly[d(A-T)$_2$]: 4.94 × 10^{-6} m and 4.90 × 10^{-6} m, respectively. The radius of poly[d(G-C)$_2$] was 4.46 × 10^{-6} m. These values correspond to approximately 1.31 ~ 1.45 × 10^4 bases, which is unrealistic.

The Stern-Volmer plot of the quenching of ethidium fluorescence with BMPyP in the presence of DNA or polynucleotide are linear (Figure 6(b)), in contrast to the TMPyP case. The smallest Stern-Volmer constant (1.60 × 10^5 M^{-1}) was obtained for DNA. The slopes of the other gave constants for poly[d(A-T)$_2$] and poly[d(G-C)$_2$] as 2.41 × 10^5 M^{-1} and 2.46 × 10^5 M^{-1}, respectively.

Resonance Energy Transfer. Although the Soret absorption band is dominant, porphyrins absorb radiation within most of the uv/visible wavelength range, thereby making them good acceptors for energy transfer. The fluorescence emission spectra of DNA- and polynucleotide-bound ethidium overlapped with the absorption spectra of the porphyrins; spectra of the ethidium-DNA-TMPyP complex are shown in Figure 8. The fluorescence emission spectrum of DNA-bound TMPyP is also shown in the same figure. Poly[d(A-T)$_2$] and poly[d(G-C)$_2$]-bound ethidium and TMPyP produced similar spectral overlap at similar concentrations. Similar results were obtained when BMPyP was used as the acceptor. The overlap integrals, $J(\lambda)$, in Equation (4), correspond to the common area under the emission spectra of ethidium and the absorption spectra of the porphyrins are summarized in Table 1. The overlap integrals of TMPyP were larger than those of BMPyP. The largest was 1.136 × 10^{-13} cm^{3}mol^{-1} for

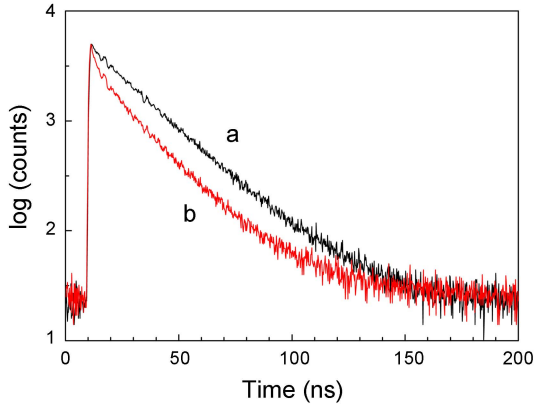

Figure 7. Sample fluorescence decay time of ethidium bound to DNA in the absence (curve a) and presence (curve b) of TMPyP. [DNA] = 100 μM, [ethidium] = 0.5 μM and [TMPyP] = 2.5 μM. The excitation and emission wavelengths were 493 and 592 nm, respectively. In this example, the fluorescence decay time of ethidium in the absence of TMPyP was 22.4 ns, and in its presence, decay times were 19.1 ns and 2.17 ns with relative amplitudes of 0.895 and 0.105, respectively.

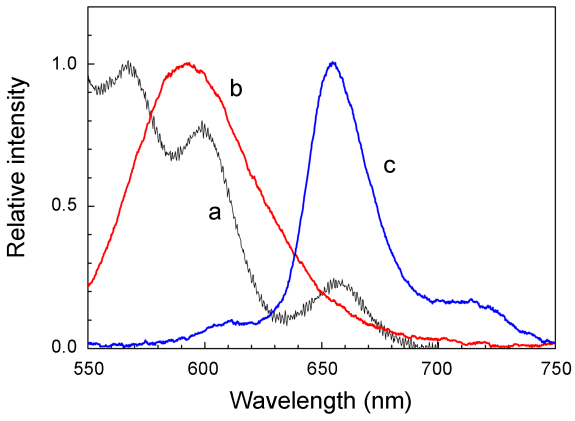

Figure 8. Rescaled absorption (curve a) and emission (curve c) spectra of the TMPyP-DNA complex and the emission (curve b) spectrum of ethidium bound to DNA in the wavelength region related to the resonance energy transfer. The maxima of all the spectra were normalized to one for ease of comparison.

Table 1. The fluorescence quantum yields of ethidium (Q_D), overlap integrals ($J(\lambda)$), orientation factor(κ)-dependent distance R_0, and efficiency of energy transfer (E) estimated from Equation (5)

Polynucleotide	Q_D	Porphyrin	$J(\lambda) \times 10^{13}$, cm^3mol^{-1}	$R_0 \times 10^7$, cm	E
DNA	0.219[a]	TMPyP	0.886	4.19 $\kappa^{1/3}$	0.543
		BMPyP	0.660	3.99 $\kappa^{1/3}$	0.286
Poly[d(A-T)$_2$]	0.216[b]	TMPyP	0.788	4.10 $\kappa^{1/3}$	0.526
		BMPyP	0.492	3.79 $\kappa^{1/3}$	0.387
Poly[d(G-C)$_2$]	0.175[b]	TMPyP	1.136	4.21 $\kappa^{1/3}$	0.425
		BMPyP	0.702	3.89 $\kappa^{1/3}$	0.371

[a]datum adopted from reference 40. [b]data were calculated from the ratios of areas under the emission spectra. [Polynucleotide] = 100 μM, [ethidium] = 0.5 μM, and [porphyrin] = 2.5 μM.

the TMPyP-poly[d(G-C)$_2$] complex and the smallest 0.492 × 10^{-13} cm^3mol^{-1} for the BMPyP-poly[d(A-T)$_2$] complex. The quantum yield, Q_D, of the DNA-bound ethidium in the absence of the porphyrins was adopted from a reported value.[40] The quantum yields of ethidium bound to poly[d(A-T)$_2$] and poly[d(G-C)$_2$] were calculated from the size of the relative area of the respective emission spectrum. The quantum yields of ethidium bound to DNA and to poly[d(A-T)$_2$] were almost identical, while that for poly[d(G-C)$_2$] was slightly lower at 0.176.

In Equation (4), the orientation factor, κ, cannot be random ($\kappa = 2/3$), because both the ethidium and porphyrin molecules are not free to rotate preventing the exact calculation of R_0. However, the orientation factor-dependent R_0 could be calculated from Equation (4) using the integral values, $J(\lambda)$, the quantum yields, Q_D, and the refractive index of for water (1.33). The resulting orientation factor-dependent Förster distances are listed in Table 1. The distances ranged from $3.79 \times 10^{-7}\kappa^{1/3} \sim 4.21 \times 10^{-7}\kappa^{1/3}$ cm, or 37.9-42.1$\kappa^{1/3}$ Å; the TMPyP-poly[d(G-C)$_2$]-ethidium complex having the longest and the BMPyP-poly[d(A-T)$_2$]-ethidium complex the shortest. Energy transfer efficiencies (Table 1) were calculated for the complexes at concentrations of [polynucleotide in base] = 100 μM, [ethidium] = 0.5 μM, and [porphyrin] = 2.5 μM using Equation (5). The distance between ethidium and porphyrin was assumed to be equal for all the complexes because no cooperative binding was found. However, the exact distance could not be obtained. The energy transfer, E, from ethidium to TMPyP was most efficient through DNA, reaching E = 0.543, while the BMPyP-DNA-ethidium complex exhibited the lowest efficiency (0.286). The efficiencies of the other complexes lied between these two extremes. There was no apparent relationship between energy transfer efficiency and Förster distance.

Discussion

Known Binding Modes of TMPyP and BMPyP. The binding modes of TMPyP and BMPyP to DNA and synthetic polynucleotides have thoroughly been investigated through spectroscopic methods, including absorption, CD and linear dichroism spectroscopies.[33,34] The large decrease in absorbance, red shift in the absorption maximum, and the negative CD band in the Soret absorption region observed for TMPyP in the presence of DNA and poly[d(G-C)$_2$] were in agreement with other works, indicating that TMPyP intercalated between the GC bases pairs in poly[d(G-C)$_2$] and DNA. With DNA, groove binding of a minority of TMPyP is also suggested. In contrast, the majority of TMPyP binds at the minor groove of poly[d(A-T)$_2$], probably across it, at the low [TMPyP]/[DNA base] ratios adopted in this work.[28] Although the binding mode of BMPyP to the native and synthetic polynucleotides was less clear,[33,34] BMPyP exhibited similar binding properties to DNA and poly[d(A-T)$_2$] that suggested stacking along the polynucleotide stem. In contrast, BMPyP bound to the outside of poly[d(G-C)$_2$]. For both TMPyP and BMPyP, the presence of ethidium at an [ethidium]/[DNA base] ratio of 0.005 did not alter the spectral properties of the polynucleotide-bound TMPyP or BMPyP, indicating independent binding of ethidium and the porphyrins to DNA and the synthetic polynucleotides, i.e., the presence of either molecule did not affect the binding properties of other.

Quenching Properties and the Inner Sphere Model. In the Stern-Volmer plot, the upward tending curves observed for TMPyP suggest the applicability of the inner sphere model (Equation (2)), with totally efficient quenching when the fluorophore and quencher were within a certain distance (sphere of action). In this equation, the dynamic quenching constant, $K_D = k_q\tau$, can be estimated from the ratio of the fluorescence decay time in the absence of TMPyP to that its presence at various concentrations. The fluorescence decay profiles of the DNA- or polynucleotides-bound ethidium were described by a single exponential decay component, while a short component appeared as the TMPyP concentration increased. The short component was likely caused by the fluorescence decay time of DNA- or polynucleotide-bound TMPyP, as a similar decay was observed in the absence of ethidium. Even if it were treated as a shortened ethidium decay time for the quenching of TMPyP, the averaged decay time remained constant, indicating that the contribution of K_D in Equation (2) was negligible. This assumption is plausible because both ethidium and porphyrin bound to DNA or polynucleotide preventing free collision between the two molecules. Based on this argument, Equation (2) was reduced to Equation (6) and from this the best-fit curve was used to determine the radii of the spheres of action. These were similar for DNA and poly[d(A-T)$_2$], corresponding 1.45×10^4 bases for the ethidium-DNA-TMPyP complex. The radii of the inner spheres corresponded to 1.45×10^4 and 1.31×10^4 bases for poly[d(A-T)$_2$] and poly[d(G-C)$_2$], respectively. These values are implausible because the lengths of the commercial synthetic polynucleotides were shorter than the inner sphere radii.

BMPyP exhibited a linear Stern-Volmer plot, suggesting that fluorescence quenching occurred through a simple static mechanism, where the fluorophore (polynucleotide-bound ethidium) formed a non-fluorescent complex with the quen-

cher (polynucleotide-bound porphyrins). In the excited state, charge separation between the fluorophore and the quencher has been suggested.[40] This observation contrasted with results from TMPyP. Neglecting the contribution from the dynamic mechanism, at least two static mechanisms could be involved in the TMPyP quenching. If charge separation were assumed in the excited state, the TMPyP results suggest the existence of at least two different states, while those from BMPyP, one.

The Förster Resonance Energy Transfer. The FRET model (equation (4)) was considered after rejection of the simple Stern-Volmer model for the quenching of the DNA- and polynucleotide-bound ethidium and porphyrins. However, in this model, the orientation factor, κ, cannot be random because both the ethidium and porphyrin molecules were not free to rotate. This prevented the exact calculation of R_0 value. The distance between ethidium and porphyrin was assumed to be independent of the nature of the base in the calculations and was the same when the concentrations of ethidium and the porphyrins were the same, e.g., the distance between ethidium and TMPyP was assumed to be the same whether they were simultaneously bound to DNA, poly[d(G-C)$_2$] or poly[d(A-T)$_2$]. TMPyP was a better quencher for all of the polynucleotides with shorter Förster distance and higher energy transfer efficiency than BMPyP. Considering that the acceptors, TMPyP and BMPyP, possessed various binding modes, binding mode was not a major factor in determining the differences in their efficiencies. The number of positive charges seemed to affect the efficiencies of TMPyP and BMPyP. Both intercalated (DNA and poly[d(G-C)$_2$] case) and minor groove binding (in poly[d(A-T)$_2$] case) TMPyP are in closed contact with nucleo-bases, while both stacked (along DNA and poly[d(A-T)$_2$] case) and outside binding (in poly[d(G-C)$_2$] case) BMPyP apart from then, which may, at least in part, contribute the efficiency differences.

For TMPyP, the Förster distances in DNA, poly[d(A-T)$_2$] and poly[d(G-C)$_2$], were $4.19\kappa^{1/3} \times 10^{-13}$, $4.10\kappa^{1/3} \times 10^{-13}$, and $4.21\kappa^{1/3} \times 10^{-13}$, respectively. Since the binding modes were similar for DNA and poly[d(G-C)$_2$] but different for poly[d(A-T)$_2$], the similar calculated transfer efficiencies of DNA and poly[d(A-T)$_2$] were surprising, as was the lowest efficiency for poly[d(G-C)$_2$]. Additionally, the orientation factor κ, was expected to be similar for DNA and poly[d(G-C)$_2$], where TMPyP was intercalated.

The appearances of the porphyrin's emission spectra in the presence and absence of ethidium were very different and depended on the nature of the polynucleotides. The large increases of emission intensity of TMPyP-poly[d(A-T)$_2$] with increasing TMPyP concentrations contrasted with the negligible or very small increases of the TMPyP-DNA and TMPyP-poly[d(G-C)$_2$] complexes. TMPyP intercalated between the nucleobases of DNA and poly[d(G-C)$_2$] and therefore, prevented the access of polar water molecule. Hence, TMPyP was located in a nonpolar environment when bound to DNA and poly[d(G-C)$_2$], but was exposured to a polar aqueous environment when bound to poly[d(A-T)$_2$]. These differences of environmental polarity and/or the accessibility of water molecules are possibly responsible for the difference in the emission intensities of TMPyP. BMPyP exhibited significant emission intensity when bound to DNA, poly[d(A-T)$_2$] and poly[d(G-C)$_2$]. The extent of the increase was largest for poly[d(A-T)$_2$]. This result can also be understood through the exposure of the porphyrin molecules to aqueous environments.

Conclusion

The energy of excited ethidium can transfer to cationic porphyrins across a large distances when both are simultaneously bound to the same DNA or polynucleotide. The number of positive charges is, at least in part, responsible for the different FRET efficiencies and the Förster distances.

Acknowledgments. This work was supported by the National Research Foundation (Grant no. 0087304 and 0083855)

References

1. Barton , J. K.; Kumar, C. V.; Turro, N. J. *J. Am. Chem. Soc.* **1986**, *108*, 6391-6393.
2. Boon, E. M.; Barton, J. K. *Curr. Opin. Struct. Biol.* **2002**, *12*, 320-329.
3. Giese, B. *Curr. Opin. Chem. Biol.* **2002**, *6*, 612-618.
4. Wagenknecht, H.-A. *Angew. Chem. Int. Ed.* **2003**, *42*, 2454-2460.
5. Wagenknecht, H.-A. *Nat. Prod. Rep.* **2006**, *23*, 973-1006.
6. Giese, B. *Med. Chem.* **2006**, *14*, 6139-6143.
7. Núñez, M. E.; Holmquist, G. P.; Barton, J. K. *Biochemistry* **2001**, *40*, 12465-12471.
8. Núñez, M. E. K.; Noyes, T.; Barton, J. K. *Chem. Biol.* **2002**, *9*, 403-415.
9. Kelly, S. O.; Jackson, N. M.; Hill, M. G.; Barton, J. K. *Angew. Chem. Int. Ed.* **1999**, *38*, 941-945.
10. Vainrub, A.; Pettitt, B. M. *Chem. Phys. Lett.* **2000**, *323*, 160-166.
11. Park, S. J.; Taton, T. A.; Mirkin, C. A. *Science* **2002**, *295*, 1503-1506.
12. Porath, D.; Cuniberti, G.; Di Felice, G. R. *Charge Transport in DNA-based Devices*; In *Topics in Current Chemistry*; Shuster, G. B., Ed.; Springer: Berlin, 2004; *237*, 183-228.
13. Schuster, G. B. *Acc. Chem. Res.* **2000**, *33*, 253-260.
14. Giese, B. *Acc. Chem. Res.* **2000**, *33*, 631-636.
15. Takada, T.; Kawai, K.; Tojo, S.; Majima, T. *Tetrahedron Lett.* **2003**, *44*, 3851-3854.
16. Kawai, K.; Kodera, H.; Osakada, Y.; Majima, T. *Nature Chem.* **2009**, *1*, 156-159.
17. Lakhno, V. D.; Sultanov, V. B.; Pettitt, B. M. *Phys. Lett.* **2004**, *400*, 47-53.
18. Rak, J.; Makowska, J.; Voityuk, A. A. *Chem. Phys.* **2006**, *325*, 567-574.
19. Sadowska-Aleksiejew, A.; Rak, J.; Voityuk, A. A. *Chem. Phys. Lett.* **2006**, *429*, 546-550.
20. Lilley, D. M. J.; Wilson, T. J. *Curr. Opin. Chem. Biol.* **2000**, *4*, 507-517.
21. Murata, S.-I.; Kuœba, J.; Gryczynski, G. I.; Lakowicz, J. R. *Biopolymers* **2000**, *57*, 306-315.
22. Kang, J. S.; Lakowicz, J. R. *J. Biochem. Mol. Biol.* **2001**, *34*, 551-558.
23. Malicka, J.; Gryczynski, I.; Fang, J.; Kusba, J.; Lakowicz, J. R. *Anal. Biochem.* **2003**, *315*, 160-169.
24. Lee, B. W.; Moon, S. J.; Youn, M. R.; Kim, J. H.; Jang, H. G.;

Kim, S. K. *Biophys. J.* **2003**, *85*, 3865-3871.
25. Yun, B. H.; Kim, J.-O.; Lee, B. W.; Lincoln, P.; Nordén, B.; Kim, J.-M.; Kim, S. K. *J. Phys. Chem. B.* **2003**, *107*, 9858-9864.
26. Youn, M. R.; Moon, S. J.; Lee, B. W.; Lee, D.-J.; Kim, J.-M.; Kim, S. K. *Bull. Korean Chem. Soc.* **2005**, *26*, 537-542.
27. Choi, J. Y.; Lee, J.-M.; Lee, H.; Jung, M. J.; Kim, S. K.; Kim, J. M. *Biophys. Chem.* **2008**, *134*, 56-63.
28. Jin, B.; Lee, H. M.; Lee, Y.-A.; Ko, J. H.; Kim, C.; Kim, S. K. *J. Am. Chem. Soc.* **2005**, *127*, 2417-2424.
29. Jin, B.; Min, K. S.; Han, S. W.; Kim, S. K. *Biophys. Chem.* **2009**, *144*, 38-45.
30. Larsen, T. A.; Goodsell, D. S.; Cascio, D.; Grzeskowiak, K.; Dickerson, R. E. *J. Biomol. Struct. Dyn.* **1989**, *7*, 477-491.
31. Vlieghe, D.; Sponer, J.; Van Meervelt, L. *Biochemistry* **1999**, *38*, 16443-16451.
32. Kim, H.-K.; Kim, J.-M.; Kim, S. K.; Rodger, A.; Nordén, B. *Biochemistry* **1996**, *35*, 1187-1194.
33. Jung, J.-A.; Lee, S. W.; Jin, B.; Sohn, Y.; Kim, S. K. *J. Phys. Chem. B* **2010**, *114*, 7641-7648.
34. Jin, B.; Ahn, J. E.; Ko, J. H.; Wang, W.; Han, S. W.; Kim, S. K. *J. Phys. Chem. B* **2008**, *112*, 15875-15882.
35. Lee, Y.-A.; Lee, S.; Cho, T.-S.; Kim, C.; Han, S. W.; Kim, S. K. *J. Phys. Chem. B* **2002**, *106*, 11351-11355.
36. Lee, Y.-A.; Kim, J.-O.; Cho, T.-S.; Song, R.; Kim, S. K. *J. Am. Chem. Soc.* **2003**, *125*, 8106-8107.
37. Kim, J.-O.; Lee, Y.-A.; Yun, B. H.; Han, S. W.; Kwag, S. T.; Kim, S. K. *Biophys. J.* **2004**, *86*, 1012-1017.
38. Ismail, M.; Rodger, P. M.; Rodger, A. A. *J. Biomol. Struct. Dyn. Conversation* **2000**, *11*, 335-348.
39. Lakowiz, J. R. *Principles of Fluorescence Spectroscopy*, 3rd ed.; Springer: New York, U.S.A., 2006.
40. Lakowicz, J. R.; Piszczek, G.; Kang, J. S. *Anal. Biochem.* **2001**, *288*, 62-75.